

## Unpolarized GPDs of sea quarks in the proton from nonlocal chiral Lagrangian

---

Fangcheng He<sup>a,\*</sup>

<sup>a</sup>*CAS Key Laboratory of Theoretical Physics, Institute of Theoretical Physics, Chinese Academy of Sciences, Beijing 100190, China*

*E-mail:* [hefc123@itp.ac.cn](mailto:hefc123@itp.ac.cn)

We calculate the unpolarized generalized parton distributions (GPDs) of sea quarks in the proton at zero skewness by using a nonlocal chiral Lagrangian. The one loop contributions from pseudoscalar mesons, intermediate octet and decuplet baryons are included. The three dimensional distribution of sea quark GPDs have been obtained. The flavor asymmetries for sea quarks at zero momentum transfer, as well as strange form factors are obtained from the GPDs. The results are comparable with phenomenological extractions and lattice QCD.

\*\*\* *Particles and Nuclei International Conference - PANIC2021* \*\*\*

\*\*\* *5 - 10 September, 2021* \*\*\*

\*\*\* *Online* \*\*\*

---

\*Speaker

## 1. Introduction

The parton distribution functions (PDFs) depict the longitudinal distribution of partons in the hadron. Compared with PDFs, Generalized Parton Distributions (GPDs) [1, 2] contain more fruitful information on the partonic structure of the nucleon, they can provide the three-dimensional distribution of partons. In addition, one can obtain the corresponding form factors by integrating GPDs with momentum fraction  $x$ .

Due to the non-perturbative property of QCD, it is very difficult to calculate GPDs from first principles. In the recent years, although quasi-PDFs [3], pseudo-PDFs [4] and lattice good cross sections [5] have been proposed, the simulation of GPDs on the Lattice is still in an early stage. Chiral perturbation theory ( $\chi$ PT) is a powerful tool to study the hadron structures in the non-perturbative region. Historically, most formulations of EFTs are based on dimensional or infrared regularisation. Though EFT is a successful and systematic approach, it is only valid for describing hadron properties at small momentum transfer [6]. In these years, we proposed a nonlocal chiral effective Lagrangian which makes it possible to study the hadron properties at relatively large momentum transfer [7, 8]. The nonlocal interaction generates the regulator which makes the loop integral convergent. The obtained electromagnetic form factors and strange form factors of the nucleon are very close to the experimental data up to  $Q^2=1 \text{ GeV}^2$ . This method also has been applied to calculate the  $\bar{d} - \bar{u}$  and  $s - \bar{s}$  flavor asymmetry in the proton [9, 10].

## 2. Splitting function and convolution formulism

The GPDs are defined by the matrix elements of bi-local field operators as

$$\int \frac{d\lambda}{2\pi} e^{-ix\lambda P^+} \langle p' | \bar{q}(\frac{\lambda n}{2}) \not{n} q(-\frac{\lambda n}{2}) | p \rangle = \bar{u}(p') \left[ \not{n} H^q(x, \xi, t) + \frac{i\sigma^{\mu\nu} n_\mu q_\nu}{2M} E^q(x, \xi, t) \right] u(p), \quad (1)$$

where  $n_\mu$  is the light-cone vector projection of the "plus" component of momenta.  $x = \frac{k^+}{P^+}$  is the quark longitudinal momentum fraction and  $P = \frac{p'+p}{2}$ .  $\xi$  is the skewness parameter defined as  $\xi = -\frac{q \cdot n}{2} = -\frac{q^+}{2P^+}$  and  $t = (p' - p)^2$ . After integrating  $x$ , the form factors can be obtained as

$$F_1^q(t) = \int_{-1}^1 dx H^q(x, \xi, t), \quad F_2^q(t) = \int_{-1}^1 dx E^q(x, \xi, t). \quad (2)$$

The combination of the above form factors can generate the electric and magnetic form factors as

$$G_E^N(t) = F_1^N(t) + \frac{t}{4m_N^2} F_2^N(t), \quad G_M^N(t) = F_1^N(t) + F_2^N(t). \quad (3)$$

We first calculate the splitting functions which are defined by the matrix elements of the vector currents at hadron level. The vertex is defined as

$$\int d^4 k \tilde{\Gamma}^\mu(k) = \langle N(p') | J^\mu | N(p) \rangle = \bar{u}(p') \left\{ \gamma^\mu F_1^N(t) + \frac{i\sigma^{\mu\nu} q_\nu}{2m_N} F_2^N(t) \right\} u(p) \quad (4)$$

where  $J^\mu$  is the electromagnetic current at hadron level and can be found in [12], and  $k$  is the internal meson momentum. The splitting functions are related to the vertex as

$$\bar{u}(p') \left\{ \gamma^+ f_j(y, t) + \frac{i\sigma^{+\nu} q_\nu}{2m_N} g_j(y, t) \right\} u(p) = \int d^4 k \tilde{\Gamma}_j^+(k) \delta(y - \frac{k^+}{P^+}) \equiv \Gamma_j^+. \quad (5)$$

For the case of zero skewness, the convolution formula for the  $H^q$  and  $E^q$  in the proton can be written as

$$H^q(x, t) \equiv H^q(x, \xi=0, t) = \sum_j \int_0^1 dy \int_0^1 dz \delta(x - yz) f_j(y, t) q_j^v(z, t), \quad (6a)$$

$$E^q(x, t) \equiv E^q(x, \xi=0, t) = \sum_j \int_0^1 dy \int_0^1 dz \delta(x - yz) g_j(y, t) q_j^v(z, t), \quad (6b)$$

where  $q_j^v(z, t)$  is the GPD of the valence quark  $q$  in the intermediate state  $j$ . The sum over  $j$  in Eqs. (6) includes both electric and magnetic couplings,  $q_j \rightarrow H_j^q$  or  $E_j^q$ . More details can be found in [12].

### 3. Numerical results

In the nonlocal chiral Lagrangian, the covariant regulator is naturally introduced to cut off the UV divergence. The covariant regulator is chosen to be of a dipole form

$$\tilde{F}(k) = \left( \frac{\Lambda^2 - m_\phi^2}{\Lambda^2 - k^2} \right)^2, \quad (7)$$

where  $m_\phi$  is the meson mass.  $\Lambda$  is chosen to be around 1 GeV as in our previous calculation for nucleon electromagnetic and strange form factors [7, 8].

The flavor asymmetry of sea quark GPDs are plotted in Fig. (1). One can see that  $xH^{\bar{d}-\bar{u}}$  and  $xE^{\bar{d}-\bar{u}}$  are both positive for all  $x$ , i.e., the values for  $\bar{d}$  are larger than  $\bar{u}$ . The  $\bar{d} - \bar{u}$  asymmetry is obvious at small  $-t$  and it decreases with increasing momentum transfer. Though the net strangeness of the nucleon is zero,  $xH^s$  is larger than  $xH^{\bar{s}}$ . For a given  $x$ ,  $xH^{s-\bar{s}}$  does not decrease monotonously with  $-t$ . The maximum asymmetry of  $xH^{s-\bar{s}}$  is at  $x$  between 0.2 and 0.3. For  $xE^{s-\bar{s}}$ , the sign changes with  $x$  and one can see that the  $s - \bar{s}$  asymmetry is much smaller than the  $\bar{d} - \bar{u}$  asymmetry in the nucleon.

The Dirac and Pauli form factors of the strange quark can be obtained from the  $x$  integrals of GPDs  $H^s(x, t)$  and  $E^s(x, t)$ . We plot the electromagnetic form factors of the strange quark in Fig. (2) which are the combinations of Dirac and Pauli form factors. The strange electric form factor versus momentum transfer  $-t$  is plotted in the left panel in Fig. (2). The upper and lower lines are for results with  $\Lambda = 1.1$  GeV and 0.9 GeV, respectively. The data with error bars are from the lattice simulation at the physical pion mass [13]. When  $t = 0$ , the value of  $G_E^s(0)$  is 0, which is in agreement with the zero strangeness of the nucleon. At finite momentum transfer, the strange electric form factor is always small and positive. It first increases and then decreases slowly with the increasing  $-t$ . The strange charge radius defined as  $\langle (r_E^s)^2 \rangle = 6 \frac{dG_E^s(t)}{dt} \Big|_{t=0}$  is  $-0.003 \text{ fm}^2$  which is not sensitive to  $\Lambda$ . As for the strange electric form factor, the absolute value of the strange magnetic form factor will increase with larger  $\Lambda$ . The strange magnetic radius defined as  $\langle (r_M^s)^2 \rangle = 6 \frac{dG_M^s(t)}{dt} \Big|_{t=0}$  is  $-0.023 \pm 0.007 \text{ fm}^2$  for  $\Lambda = 1 \pm 0.1$  GeV. Our results are also consistent with the direct calculation of the strange form factors with a nonlocal chiral Lagrangian [8].

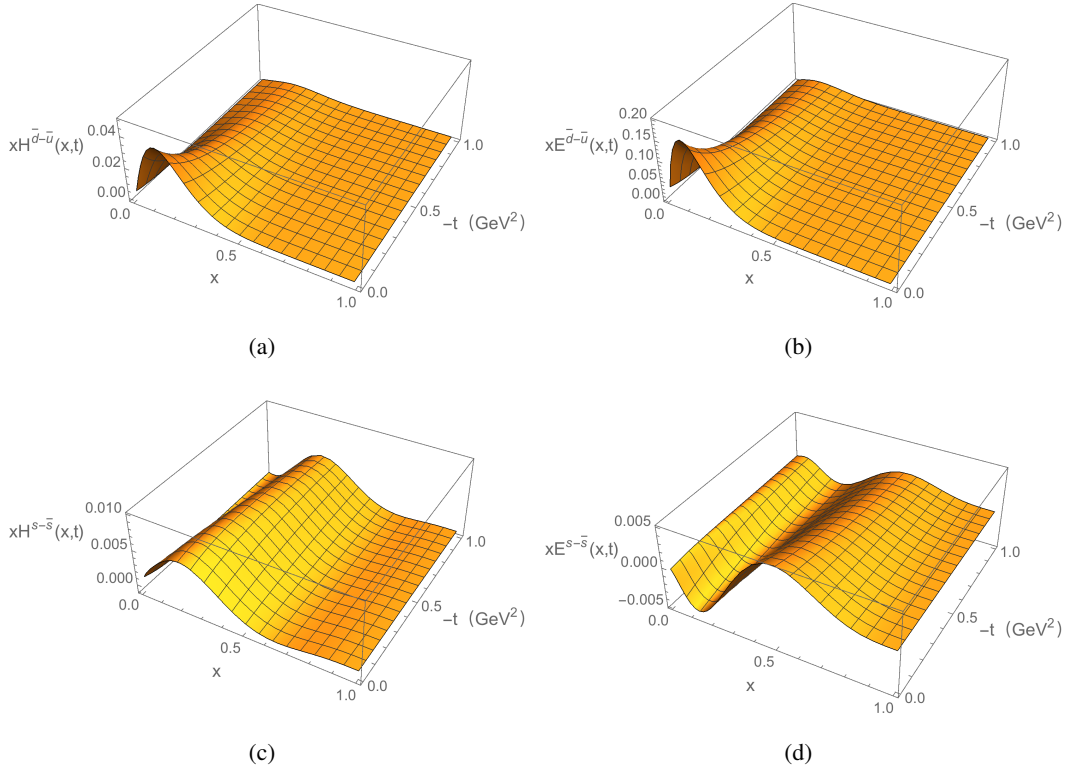


**Figure 1:** The 3D GPDs  $xH^{\bar{d}-\bar{u}}$ ,  $xE^{\bar{d}-\bar{u}}$ ,  $xH^{s-\bar{s}}$  and  $xE^{s-\bar{s}}$  versus momentum fraction  $x$  and momentum transfer  $-t$  with  $\Lambda = 1$  GeV. The corresponding scale is  $\mu^2 = 1$  GeV<sup>2</sup>.

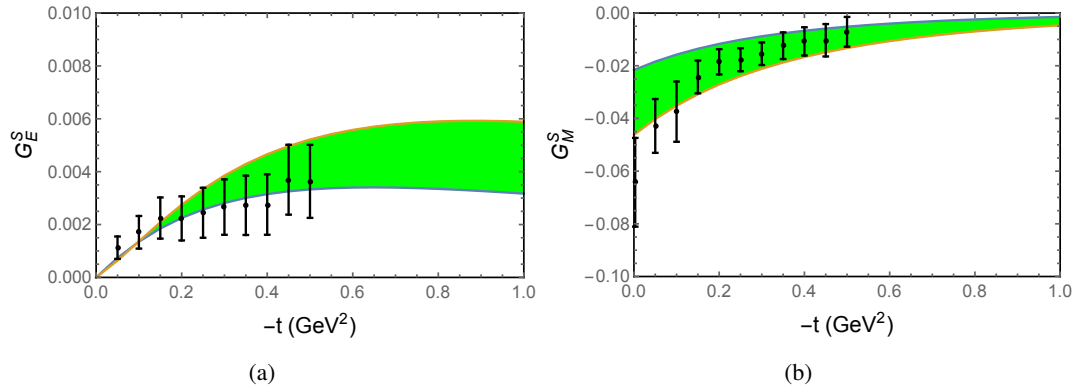


**Figure 2:** The strange electric form factor (left panel) and magnetic form factor (left panel) of proton versus momentum transfer  $-t$  with  $0.9 \leq \Lambda \leq 1.1$  GeV. The data with error bars are the results of Lattice simulation [13].

## References

- [1] X. D. Ji, Phys. Rev. D **55** (1997), 7114-7125 doi:10.1103/PhysRevD.55.7114 [arXiv:hep-ph/9609381 [hep-ph]].
- [2] X. D. Ji, J. Phys. G **24** (1998), 1181-1205 doi:10.1088/0954-3899/24/7/002 [arXiv:hep-ph/9807358 [hep-ph]].
- [3] X. Ji, Phys. Rev. Lett. **110** (2013), 262002 doi:10.1103/PhysRevLett.110.262002 [arXiv:1305.1539 [hep-ph]].
- [4] K. Orginos, A. Radyushkin, J. Karpie and S. Zafeiropoulos, Phys. Rev. D **96** (2017) no.9, 094503 doi:10.1103/PhysRevD.96.094503 [arXiv:1706.05373 [hep-ph]].
- [5] Y. Q. Ma and J. W. Qiu, Phys. Rev. D **98** (2018) no.7, 074021 doi:10.1103/PhysRevD.98.074021 [arXiv:1404.6860 [hep-ph]].
- [6] T. Fuchs, J. Gegelia and S. Scherer, J. Phys. G **30** (2004), 1407-1426 doi:10.1088/0954-3899/30/10/008 [arXiv:nucl-th/0305070 [nucl-th]].
- [7] F. He and P. Wang, Phys. Rev. D **97** (2018) no.3, 036007 doi:10.1103/PhysRevD.97.036007 [arXiv:1711.05896 [nucl-th]].
- [8] F. He and P. Wang, Phys. Rev. D **98** (2018) no.3, 036007 doi:10.1103/PhysRevD.98.036007 [arXiv:1805.11986 [hep-ph]].
- [9] Y. Salamu, C. R. Ji, W. Melnitchouk, A. W. Thomas and P. Wang, Phys. Rev. D **99** (2019) no.1, 014041 doi:10.1103/PhysRevD.99.014041 [arXiv:1806.07551 [hep-ph]].
- [10] Y. Salamu, C. R. Ji, W. Melnitchouk, A. W. Thomas, P. Wang and X. G. Wang, Phys. Rev. D **100** (2019) no.9, 094026 doi:10.1103/PhysRevD.100.094026 [arXiv:1907.08551 [hep-ph]].
- [11] R. S. Towell *et al.* [NuSea], Phys. Rev. D **64** (2001), 052002 doi:10.1103/PhysRevD.64.052002 [arXiv:hep-ex/0103030 [hep-ex]].
- [12] F. He, C. R. Ji, W. Melnitchouk, A. W. Thomas and P. Wang, [arXiv:2202.00266 [hep-ph]].
- [13] R. S. Sufian, Y. B. Yang, J. Liang, T. Draper and K. F. Liu, Phys. Rev. D **96** (2017) no.11, 114504 doi:10.1103/PhysRevD.96.114504 [arXiv:1705.05849 [hep-lat]].